

<https://revistas.ucr.ac.cr/index.php/ingenieria/index>
www.ucr.ac.cr / ISSN: 2215-2652

Ingeniería

Revista de la Universidad de Costa Rica
JULIO/DICIEMBRE 2025 - VOLUMEN 35 (2)



Frames with Intentionally Eccentric W-Shape, C-Shape, and Round HSS Braces

Marcos con riostras intencionalmente excéntricas con sección W, sección C y HSS redonda

Andrés González Ureña

Universidad de Costa Rica, San José, Costa Rica.

Professor, School of Civil Engineering and Earthquake Engineering Laboratory, San José, Costa Rica.

correo: andres.gonzalezurena@ucr.ac.cr

Keywords:

Braces with Intentional Eccentricity (BIEs), earthquake-resistant design, Frames with Intentionally Eccentric Braces (FIEBs), Non-Linear Response History Analysis (NLRHA), steel braced frames.

Abstract

Steel Frames with Intentionally Eccentric Braces (FIEBs) are an innovative Seismic Force-Resisting System (SFRS) that offers significant advantages compared to Concentrically Braced Frames (CBFs).

Recent research has shown that the adjustable stiffness and strength of Braces with Intentional Eccentricity (BIEs) with square Hollow Structural Section (HSS) bracing members allows for a better control over the structure's dynamic response and for a reduction of the capacity-based design forces on the non-energy-dissipating members.

In this article, the aptness of W-shapes, C-shapes, and round HSSs to be employed as bracing members in multi-story FIEBs is evaluated preliminarily. To this end, hypothetical buildings with FIEBs based on the three section types as their SFRS are designed using a displacement-based procedure for the seismic hazard of locations in Costa Rica, and their performance is assessed numerically with Non-Linear Response History Analysis (NLRHA).

The results show that the three section types produce FIEBs that display a satisfactory seismic response in terms of maximum story drifts and story shears, and that the use of W-shape BIEs results in the most cost-effective designs.

Recibido: 14/01/2025

Aceptado: 30/05/2025

Palabras claves:

Análisis no lineal dinámico, diseño sismorresistente, marcos arriostrados de acero, marcos con riostras intencionalmente excéntricas, riostras intencionalmente excéntricas.

Resumen

Los marcos de acero con riostras intencionalmente excéntricas (FIEB, del inglés *Frame with Intentionally Eccentric Braces*) constituyen un sistema sismorresistente novedoso que ofrece ventajas significativas en comparación con los marcos arriostrados concéntricamente.

Investigaciones recientes han mostrado que la ajustabilidad de la resistencia y la rigidez que ofrecen las riostras intencionalmente excéntricas (BIE, del inglés *Brace with Intentional Eccentricity*) de sección estructural hueca (HSS, del inglés *Hollow Structural Section*) rectangular permite un mejor control sobre la respuesta dinámica de la estructura y reducir las fuerzas de diseño por capacidad para los miembros no disipadores de energía.

En este artículo, se evalúa preliminarmente la aptitud de las secciones W, secciones C y HSS redondas para ser empleadas como BIE en FIEB de varios niveles. Con este fin, se diseñan edificios hipotéticos de diferentes alturas con FIEB basados en los tres tipos de sección mencionados, utilizando un procedimiento de diseño basado en desplazamientos y considerando la amenaza sísmica de sitios en Costa Rica. El desempeño de los edificios se evalúa numéricamente mediante análisis no lineal de respuesta en el tiempo.

Los resultados muestran una respuesta sísmica satisfactoria por parte de los FIEB con las tres secciones consideradas, en términos de razones de deriva máxima y cortantes de piso, e indican que, entre estas, las secciones W permiten diseños más eficientes.

DOI: 10.15517/ri.v35i2. 63456



NOMENCLATURE

BIE.....	Brace with Intentional Eccentricity.
CLB.....	Centrally Loaded Brace.
SFRS.....	Seismic Force-Resisting System.
CBF.....	Centrally Braced Frame.
FIEB.....	Frames with Intentionally Eccentric Braces.
HSS.....	Hollow Structural Section.
NLRHA.....	Non-Linear Response History Analysis.
e	Eccentricity.
K_i	Initial stiffness.
T_y	First-yield force.
δ_y	First-yield displacement.
T_u	Ultimate yield force.
δ_u	Ultimate yield displacement.
A	Cross-sectional area.
F_y	Yield stress.
L	Overall BIE length.
L_{ea}	<i>Eccentering</i> assemblies' length.
T	Fundamental mode period.
S_a	Spectral acceleration.
S_d	Spectral displacement.
K_s	Post-elastic stiffness.
C^*	Compressive resistance.
δ_{C^*}	Displacement at compressive resistance.
R_y	Probable yield stress modification factor.
MMPR.....	Modal Mass Participation Ratio.
η	Seismic mass to tonnage ratio.
GM.....	Ground Motion record.
RotD100.....	Maximum spectral acceleration in any direction of the ground motion.

I. INTRODUCTION

Braces with Intentional Eccentricity (BIEs) are a recently introduced type of steel brace, proposed as an alternative to Traditional Centrally Loaded braces (CLBs) in Seismic Force-Resisting Systems (SFRSs) [1]. Experimental results show that the intentional eccentricity, that is, the offset between the frame diagonal and the bracing member's axis, results in a response to loading that combines flexural and axial stresses. It also enables BIEs to overcome several shortcomings of CLBs, specifically those related to their invariably large elastic stiffness in tension, their limited post-yielding stiffness, and their susceptibility to low cycle fatigue-induced fracture [1], [2].

Moreover, when employed in multi-story Frames with Intentionally Eccentric Braces (FIEBs), the adjustable eccentricity of BIEs grants the designer a tight control over the seismic response of the structure, as it allows to provide with precision the stiffness and strength required at each story to satisfy earthquake loading demands. Numerical studies have shown that, compared with Centrally Braced Frames (CBFs), FIEBs with square Hollow Structural Section (HSS) BIEs offer an improved performance in terms of maximum and residual story drifts and may require less material [3], [4]. The typical arrangement of a FIEB in chevron with middle column configuration, as considered in [3], [4], is presented in Fig. 1.

Although the available information on FIEBs shows that the system has the potential to be recognized by seismic codes and eventually adopted by the construction industry, further investigation is required before it reaches an implementable stage. One of the various matters that must be addressed is the verification of the aptness of sections other than square HSSs to be employed as the bracing members of BIEs in FIEBs.

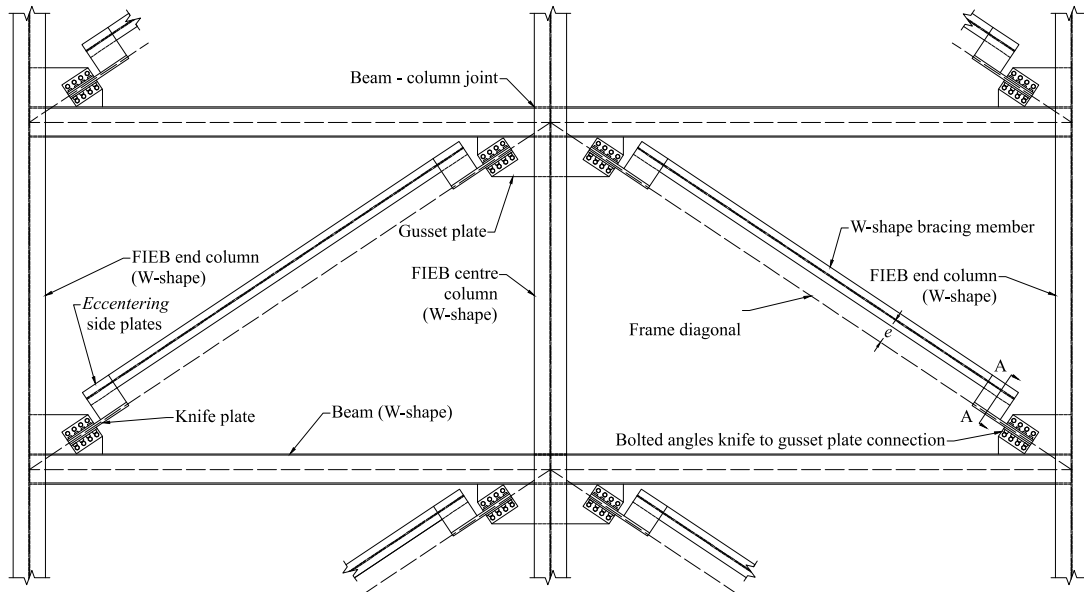


Fig. 1. Typical arrangement of a FIEB in chevron with middle column configuration (W-shape bracing members shown).

In this article, the aptness of W-shapes, round HSSs, and C-shapes for use as bracing members in FIEBs is assessed preliminarily. To this purpose, the structural design of hypothetical 4-, 8-, and 12-story buildings is carried out applying the displacement-based procedure described in [3] for the seismic hazard of locations in Costa Rica, with FIEBs based on the considered section types as their SFRS.

The performance of the resulting FIEBs is then evaluated numerically through Non-Linear Response History Analysis (NLRHA), employing ground motion records selected and scaled to be consistent with the local seismic setting and the design seismic hazard. The maximum and residual story drifts and maximum story shears are reported as indicators of the overall seismic response of the FIEBs.

II. BASIC PROPERTIES OF BIES

The basic components of a BIE and its idealized kinematic response to monotonic loading are described in Fig. 2. The eccentricity, e , is defined as the distance between the bracing member's axis and the line of action of the forces, typically the braced frame diagonal.

The eccentricity is accommodated by the *eccentering* assemblies, that is, plate arrangements which are also responsible for transmitting the forces between the ends of the bracing member and the connection of the BIE to the beam-column joint. Depending on the bracing member section and particular requirements, as discussed below, the *eccentering* assemblies may be constructed in various ways.

The connections between the BIE and the beam-column joint are idealized as pins that act as pivots for the *eccentering*

assemblies; as such, the detailing of the connection employed in practice must be coherent with this behavior. The idealized force-deformation response to monotonic tension and compression loading of BIEs is presented in Fig. 3. Under tension, the BIE responds by elongating while bending towards the frame diagonal, thus reducing the effective eccentricity at mid-span, as shown in Fig. 2(b). For small displacements, the axial response of the BIE is elastic, and can be characterized by the initial stiffness, K_i , indicated in Fig. 3(a).

Given the presence of flexural stresses, yielding initiates in the extreme fiber in tension at the “first-yield” point (T_y, δ_y), which marks the transition from the elastic to the post-elastic phases of the BIE's response to loading in tension. If the tension loading continues, yielding progresses through the cross section until it becomes completely plasticized, reaching the ultimate yield point (T_u, δ_u). The ultimate yield force, T_u , is equal to the product of the cross-sectional area, A , and the yield stress, F_y , and corresponds to the tensile strength of a CLB of same cross-section. To reach this stage, however, the eccentricity must be annulled along the bracing member's length, which may require the development of plastic hinges where the bracing member meets the eccentering assemblies, as illustrated in Fig. 2(c).

The rotation demand at the bracing member's ends depends on the eccentricity, the overall length, L , and the *eccentering* assemblies' length, L_{ea} , as explained in [2]. The effective axial stiffness during the post-elastic phase of the BIE's response to loading is variable, as it depends on the instantaneous deformed configuration of the system; however, the average post-elastic stiffness, K_s , can be used to characterize this phase and to construct a simplified trilinear backbone curve describing the BIE's response to tension loading, as shown with the dotted line in Fig. 3(a).

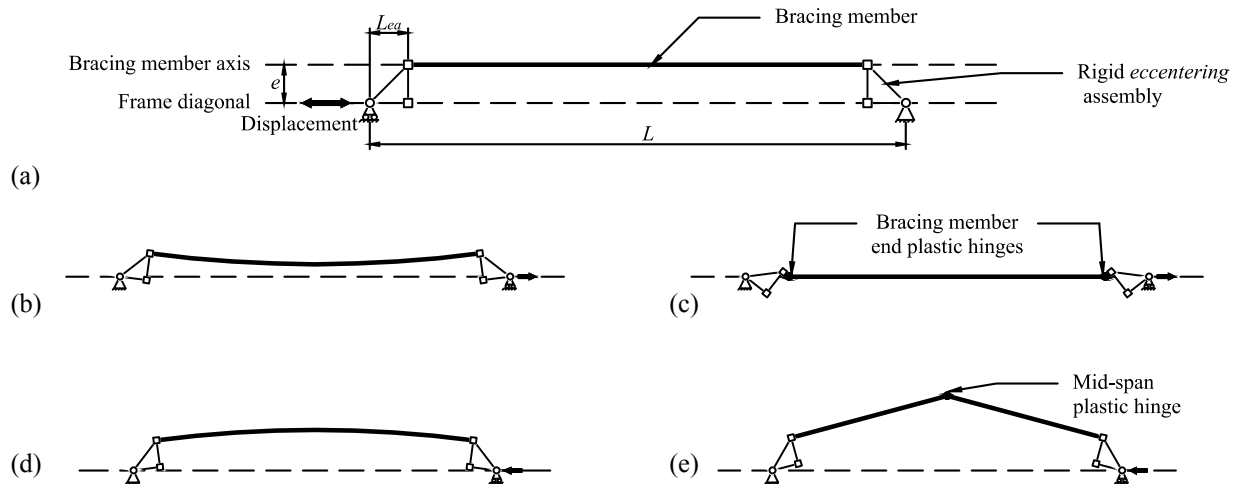


Fig. 2. Basic components of a BIE and kinematic response to loading: (a) components and dimensions, (b) deformed shape under small displacement in tension, (c) deformed shape under large displacement in tension, (d) deformed shape under small displacement in compression, and (e) deformed shape under larger displacement in compression.

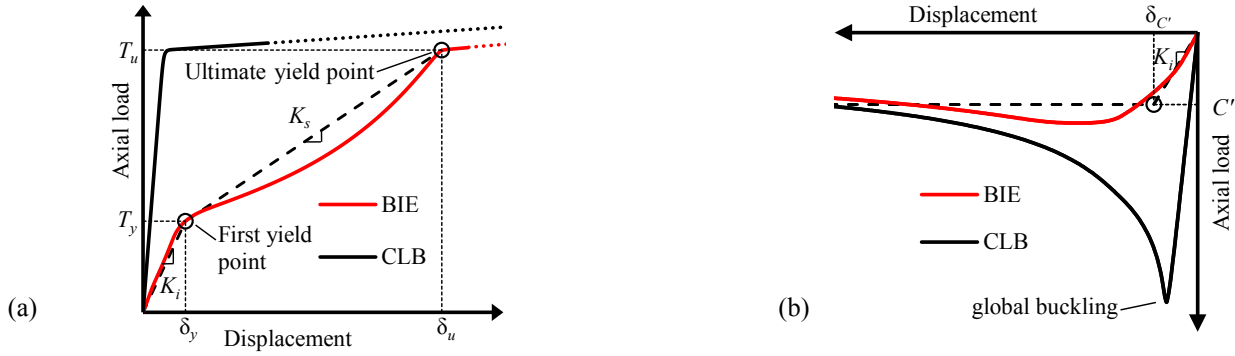


Fig. 3. Idealized monotonic force-deformation response: (a) tension loading and (b) compression loading.

It can be noted that the trilinear response to tension loading of BIEs, with its significant post-yielding stiffness, is markedly different to the equivalent response of CLB, consistent with an elastic-perfectly plastic model.

Under compression loading, the BIE shortens and bends away from the frame diagonal, as presented in Fig. 2(d). Given the flexural nature of its response, the BIE does not buckle as a CLB and is able to sustain a load close to its maximum resistance at large displacements. As such, the response of BIEs under monotonic compression can be approximated by an elastic-perfectly plastic model with elastic stiffness K_i and compressive resistance C' , as presented in Fig. 3(b).

If the compression loading is sustained, a plastic hinge inevitably forms at mid-span; however, this occurs at larger displacements than in CLBs due to the flexural demands inducing a more even distribution of strain demands over the length of the bracing member, as discussed in [1],[2]. This delay in the development of the mid-span plastic hinge implies a delay in

the onset of local buckling and, thus, renders BIEs capable of sustaining larger deformations than CLBs before becoming at risk of a low cycle fatigue-induced fracture.

How eccentricity affects the response of BIEs as individual members and in pairs is illustrated in Fig. 4. As can be observed in Fig. 4(a), the magnitude of both elastic and post-yielding stiffness in tension, K_i and K_s , decreases as eccentricity increases. In consequence, the load at first yield, T_y , also decreases with increasing eccentricity, and the ultimate yield force, T_u , is attained at larger displacements, δ_u .

Under compression, both the elastic stiffness and the compressive resistance, C' , decrease with the increment of eccentricity, as shown in Fig. 4(b). In Fig 4(c), the response of a pair of BIEs acting in tandem, one in tension and one in compression, is presented in terms of story shear vs. story horizontal displacement or drift. It can be noted that, for large enough eccentricities, the shape of the resulting curves is consistent with that of the response under monotonic tension, and that the effective stiffness is strictly

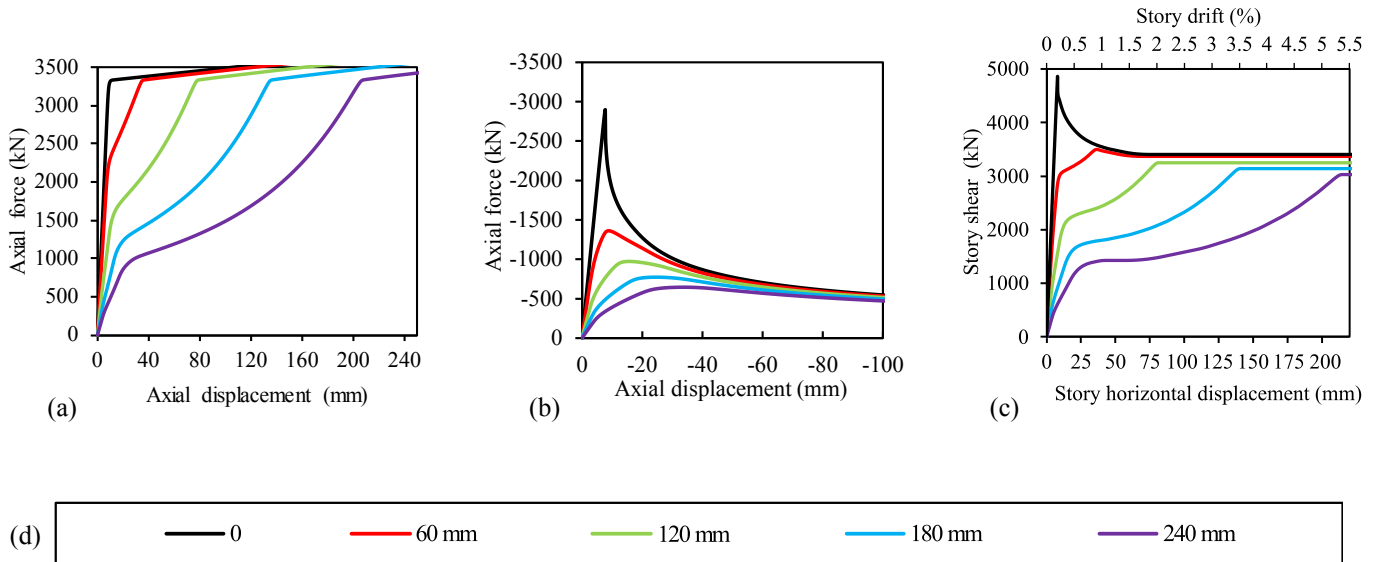


Fig. 4. Influence of eccentricity on the monotonic response of HSS 178x178x16 BIEs with $L = 5408$ mm and $Le_a = 360$ mm: (a) tension loading, (b) compression loading, (c) story shear vs. horizontal displacement of a pair of BIEs acting in tandem, and (d) magnitude of eccentricity color code.

positive, contrasting with the response of the pair of CLBs (null eccentricity), which displays a marked peak and subsequent strength loss due to buckling of the compression brace. A detailed report on the general properties of BIEs and on the response of square HSS BIEs to monotonic and cyclic loading is available in [3]. The response of W-shape, C-shape, and round HSS BIEs as individual members is described thoroughly in [5], [6], and [7], respectively, based on numerical models.

The general behavior herein described is common to BIEs with any of the considered section types; however, the magnitude of the elastic and post-elastic stiffnesses, first-yield force, and compressive resistance, depends on each BIE's particular combination of cross-section, eccentricity, overall length, L , and length of centering assemblies, L_{ea} .

III. DESIGN OF FIEBS

Traditional force-based design methods, such as those typically employed in the design of CBFs and other conventional steel SFRSs, are not compatible with FIEBs. As noted in the previous section, depending on the eccentricity, BIEs may attain their maximum strength at displacements far greater than those associated with the allowable drift limits imposed by modern design codes. Thus, designing for BIEs to attain their ultimate yield strength would imply excessive displacement and rotation demands on non-structural components. Displacement-based design methods, on the other hand, appear as an alternative well suited for FIEBs, as numerical models can be employed to easily determine the story shear developed by a pair of BIEs as a function of imposed displacement. In [3], a design procedure for FIEBs based on the Direct Displacement-Based Design method proposed

by Priestley *et al.* [8] is presented and described in detail; this procedure is employed herein to design FIEBs with BIEs with W-shape, C-shape, and round HSS bracing members.

The plan configurations of the considered buildings are presented in Fig. 5. The study focuses on the frames aligned with the longest side of the buildings. As C-shape members are significantly more flexible than W-shape or round HSS members, and as the maximum size of commercially produced C-shape sections is limited, it was necessary to select a plan configuration with shorter spans and smaller areas tributary to the braced frames for the FIEBs with C-shape BIEs. This in order to produce design outcomes that satisfy the structural demands.

The gravity loads considered in design are provided in TABLE I. In the case of the FIEBs with W-shape and round HSS BIEs, it was assumed that self-supported exterior walls would be employed. As such, although their mass participates in the seismic response of the buildings, they do not transmit load to the structural framing. In the design of the FIEBs with C-shape BIEs, the dead load corresponding to the exterior walls was combined with the roof and floor dead loads and evenly distributed over the floor plan.

The design seismic acceleration spectra were constructed as per the 2010 Costa Rican Seismic Design Code (CSCR) [9]. To this effect, the FIEBs with W-shape and round HSS BIEs were assumed located in San José, San José, thus in seismic zone III in CSCR, while for the FIEBs with C-shape BIEs a location in Nicoya, Guanacaste, (seismic zone IV) was selected. In both cases, it was supposed that the buildings would sit on soft to moderately stiff clay soil, corresponding to a site type S3 in CSCR. The resulting acceleration spectra and the displacement spectra derived from these are presented in Fig. 6.

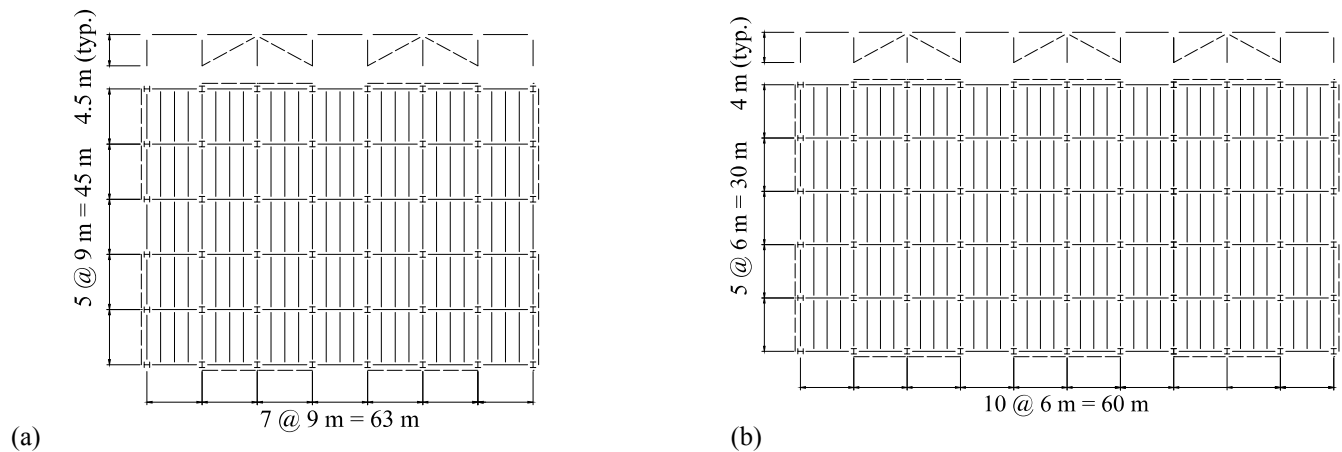


Fig. 5. Plan configuration of the buildings: (a) FIEBs with W-shape and round HSS BIEs and (b) FIEBs with C-shape BIEs.

TABLE I
GRAVITY LOADS CONSIDERED IN DESIGN

Fiebs with W-shape and round HSS BIEs		FIEBs with C-shape BIEs	
Roof	Dead = 1.65 kPa	Roof	Dead = 1.65 kPa
	Live = 0.98 kPa		Live = 0.98 kPa
Floors	Dead = 3.8 kPa	Floors	Dead = 3.8 kPa
	Live = 2.45 kPa		Live = 2.45 kPa
Exterior walls	Dead = 1.5 kPa	Exterior walls	Dead = 1.5 kPa

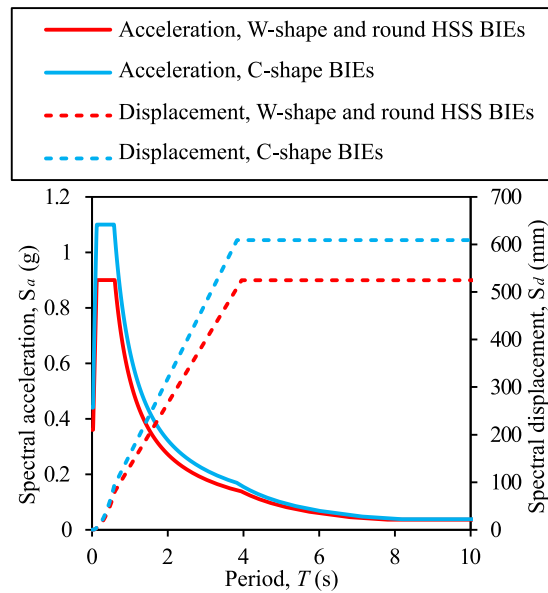


Fig. 6. Design acceleration and displacement spectra.

The chevron with a middle column arrangement adopted for the FIEBs in this study is shown in Fig. 1. For all buildings, ASTM A992 [10] W-shape sections were considered for beams and columns and ASTM A572 Gr. 50 [11] plates were considered for the connection elements and *eccentering* assemblies. The columns are oriented with their webs normal to the plane of the frame. The typical configurations of the *eccentering* assemblies employed for each of the three FIEB types are presented in Fig. 7. In the case of the W-shape and C-shape BIEs, the eccentricity is introduced by means of side plates welded to the flanges of the bracing member, which is oriented to bend about its weak axis to deter lateral torsional buckling.

The side plates are then connected to a knife plate, which in turn is connected with bolted angles to a gusset plate welded to the beam-column joint (Fig. 7(a) and 7(c)). As side plates cannot easily be welded to the sides of a round HSS, a stiffened end plate *eccentering* assembly is used instead, as shown in Fig. 7(b). Rib stiffeners are used to reinforce the connection between the HSS and the end plate to prevent fracture under tension loading as reported in [1]. The knife plates are designed to yield in flexure at low axial forces, thus emulating the pinned end behavior described above. The braced frame and connection configuration was selected to constrain the deformation of the BIEs to the plane of the frame.

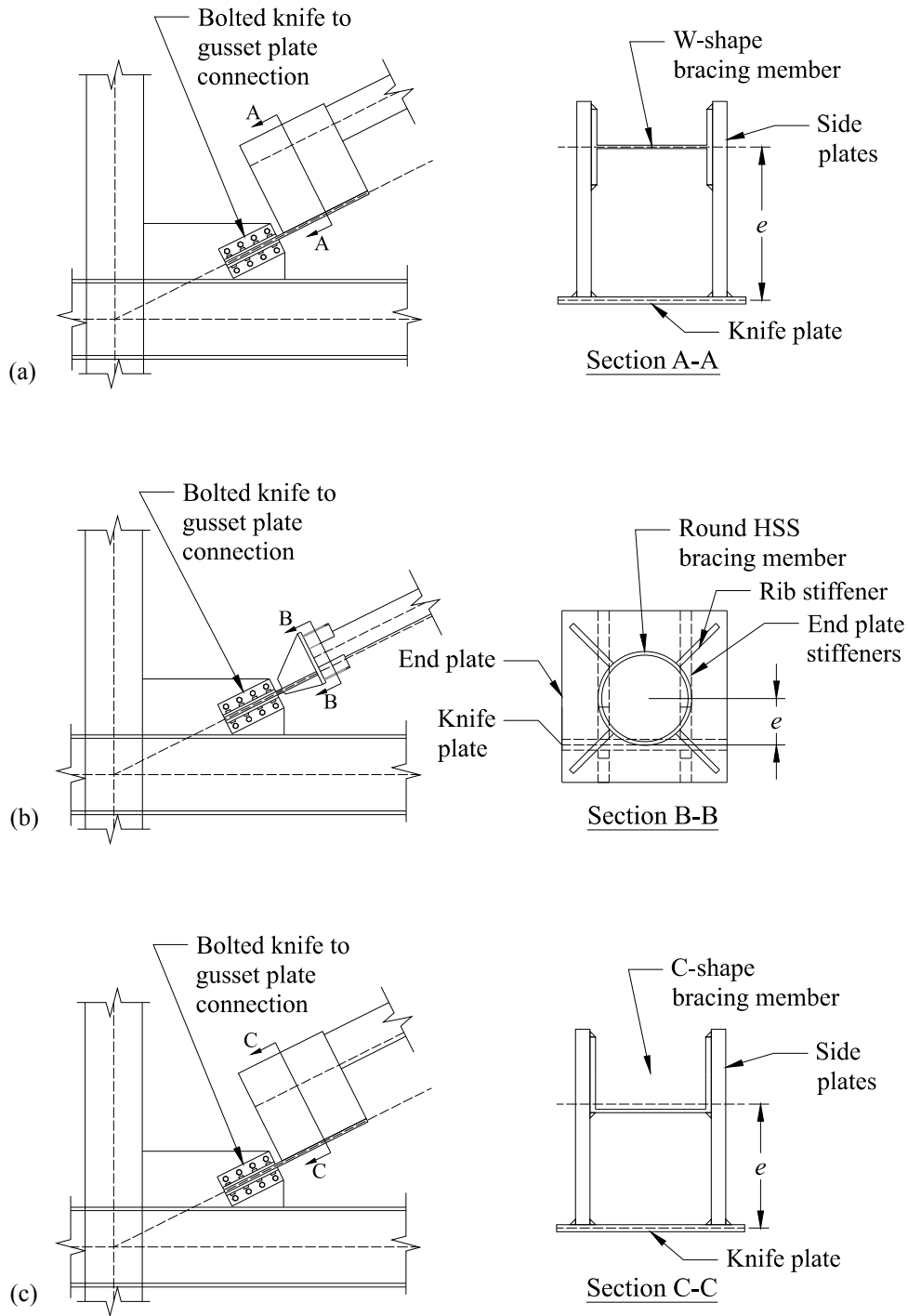


Fig. 7. Typical configurations of eccentric assemblies considered in design: (a) W-shape BIEs, (b) round HSS BIEs, and (c) C-shape BIEs.

The design of the FIEBs required as a first step the creation of databases comprising idealized axial displacement vs. force curves of every pertinent section-eccentricity combination for the three considered section types. To this end, fiber section-based finite element models of BIEs with dimensions consistent with those of the selected buildings were constructed in OpenSees [12], as detailed in [5],[6], [7].

All W-shapes, C-shapes and round HSSs listed in the *AISC Steel Construction Manual*, 16th ed. [13] complying with the highly ductile members local slenderness limits of ANSI/AISC 341-22 [14] were included in the database. The W-shapes and round HSSs were supposed to be fabricated as per the ASTM A992 [10] and ASTM A1085 [15] standards, respectively, while the C-shapes were assumed to be made from ASTM A36 steel [16]. The models for the design database considered nominal yield strength, that is, $F_y = 345$ MPa for W-shapes and round HSSs and $F_y = 250$ MPa for C-shapes. Eccentricities up to twice the section height in 5 mm increments were considered. Although the drift ratio limit for braced structures in CSCR is 1.0%, all FIEBs in this study were designed for a target drift ratio of 2.0%. This value was selected considering three factors: 1) the design procedure incorporates material non-linearity and $P-\Delta$ effects; 2) the applicable drift limits for braced frames in other design codes such as ASCE 7-22 [17] and NBCC 2020 [18] is 2.5%; and 3) the results presented in [3],[4] indicate that FIEBs are more cost-effective if designed for larger drift ratios. The design was performed for the load combinations from CSCR, while the verification of member and connection strength was carried out as per ANSI/AISC 360-22 [19]. As explained in [4], the capacity-based design forces considered in the design of the non-dissipating members of the frame, i.e., beams and columns, were calculated assuming maximum drift ratios 25% larger than the target and probable yield strength, $R_y F_y$, for the braces. The sections selected for the beams and columns in all FIEBs also complied with the highly ductile member local slenderness limits as it was deemed reasonable to apply the same requirement that ANSI/AISC 341-22 [14] imposes for these members in Special Concentrically Braced Frames (SCBFs).

The design procedure requires as input an estimation of the average equivalent damping ratio resulting from the inelastic action of the BIEs under the design seismic demands. However, as there are no available models to estimate the equivalent viscous damping produced by BIEs with the sections considered in this study, it was necessary to define initial trial values based on the data for square HSS BIEs presented in [3] and then verify

their correspondence with the actual equivalent damping ratios displayed by the BIEs selected in the final design. It was found that, for the FIEBs included in the study, an estimated equivalent damping ratio of 17.5% produced adequate results.

In TABLE II, the first mode period and modal mass participation ratio (MMPR) of the buildings designed in this study are presented, along with the approximate tonnage of steel required per braced frame. A direct assessment of the impact on cost-effectiveness of using one or other type of section for the BIEs is not possible given that the design loads and plan configuration of the FIEBs with C-shape BIEs are different than those considered in the design of the other FIEBs. Thus, to provide a relative index of cost-effectiveness, the ratios of total seismic mass tributary to a single braced frame and its tonnage, represented herein as η , are also provided in TABLE II. Note that higher values of η indicate greater cost-effectiveness.

Overall, the designed FIEBs are considerably flexible structures, as their fundamental period indicates. For reference, note that the fundamental periods of 12-, 8-, and 4-story CBFs can be estimated as 0.97 s, 0.72 s, and 0.43 s, respectively, with the equation for the approximate fundamental period proposed in ASCE 7-22 [17], or as 1.35 s, 0.9 s, and 0.45 s, with that given in NBCC 2020 [18]. The large periods of FIEBs imply that they are subjected to lower spectral accelerations than equivalent CBFs and, thus, to lower seismic forces. Moreover, it can be noted that the MMPR of the first mode decreases significantly with the number of stories for all FIEBs, which means that higher mode effects have an important weight in their dynamic response and should be considered in design, as further discussed below.

The tributary seismic mass to steel tonnage ratio, η , evidences that the cost-effectiveness of FIEBs decreases with the number of stories, which is mainly a consequence of the exponential increment on the axial loads on the columns, and that, among the three considered section types, W-shapes result in the most cost-effective FIEBs. Two factors can explain the latter observation. Firstly, the array of commercially available W-shapes complying with seismic local slenderness limits is much larger and of greater variety in sizes than those of the other two considered sections, which results in lower incidental overstrength. Secondly, the R_y factor applicable for ASTM A992 W-shapes, 1.1, is considerably lower than those corresponding to ASTM A1085 HSSs and for ASTM A36 steel C-shapes, 1.25 and 1.3, respectively. Both factors favor lower capacity-based design forces in FIEBs with W-shape BIEs and, thus, lighter sections for beams and columns.

TABLE II
FUNDAMENTAL MODE PROPERTIES AND SFRS TONNAGE OF FIEBS

FIEB	Fundamental mode properties		SFRS tonnage (t)			Seismic mass to steel tonnage ratio
	T (s)	MMPR	Braces	Beams and columns	Total	η (kN/t)
W-shape BIEs, 12-story	2.99	0.756	19.51	60.03	79.53	477.26
Round HSS BIEs, 12-story	2.36	0.759	19.09	80.54	99.63	380.98
C-shape BIEs, 12-story	2.96	0.796	8.72	31.46	40.19	434.71
W-shape BIEs, 8-story	2.28	0.808	8.02	29.30	37.32	661.40
Round HSS BIEs, 8-story	1.36	0.805	9.33	51.97	61.30	402.67
C-shape BIEs, 8-story	1.79	0.863	5.82	22.87	28.67	401.46
W-shape BIEs, 4-story	1.33	0.902	2.62	13.31	15.93	716.29
Round HSS BIEs, 4-story	1.06	0.854	3.81	15.47	19.28	591.83
C-shape BIEs, 4-story	1.13	0.916	2.60	8.04	10.63	522.01

IV. NON-LINEAR RESPONSE HISTORY ANALYSIS

The seismic performance of the FIEBs designed in this study is assessed numerically through NLRHA, in order to evaluate the response of the structures subjected to realistic earthquake demands consistent with the seismic hazard considered in design. In this section, aspects regarding the selection and scaling of the ground motion records employed in the analysis and numerical modelling are discussed

A. Ground motion records selection and scaling

The ground motion records employed in the NLRHA were selected and scaled following the guidelines of ASCE 7-22 [17] with the design acceleration spectra set as target, in order to be representative of the actual seismic hazard at the hypothetical locations of the buildings. According to the seismic hazard deaggregation presented in [20], [21], in San José, crustal

earthquakes from nearby faults govern the seismic hazard for periods lower than 1.0 s, while for longer periods, subduction earthquakes occurring in the plate interface along the Pacific coast account for most of the hazard.

In Nicoya, the seismic hazard is predominated by subduction earthquakes for all periods. Therefore, for the FIEBs with W-shape and round HSS BIEs in San José, a suite comprising a set of eleven crustal ground motion records (GMs), scaled for a period range from 0.25 s to 2.0 s, and eleven subduction GMs, scaled for periods ranging from 1.0 s to 6.0 s, was prepared. For the FIEBs with C-shape BIEs in Nicoya, another set of eleven subduction GMs, scaled for periods between 0.25 s and 6.0 s was prepared. The crustal GMs were obtained from the PEER NGA West 2 database [22], and the subduction GMs were provided by the K-NET and KiK-net databases [23]. In Fig. 8 and Fig. 9, the RotD100 response spectra of the GM suites employed in the NLRHA are shown, and TABLE III lists the GMs included in the NLRHA along with their associated final scale factors.

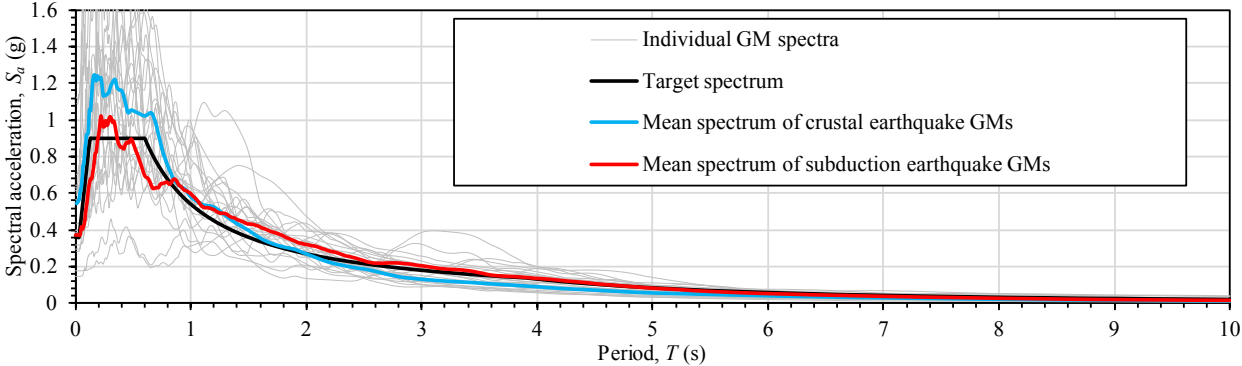


Fig. 8. Response spectra of the ground motions used in the NLRHA of the FIEBs with W-shape and round HSS BIEs.C-shape BIEs.

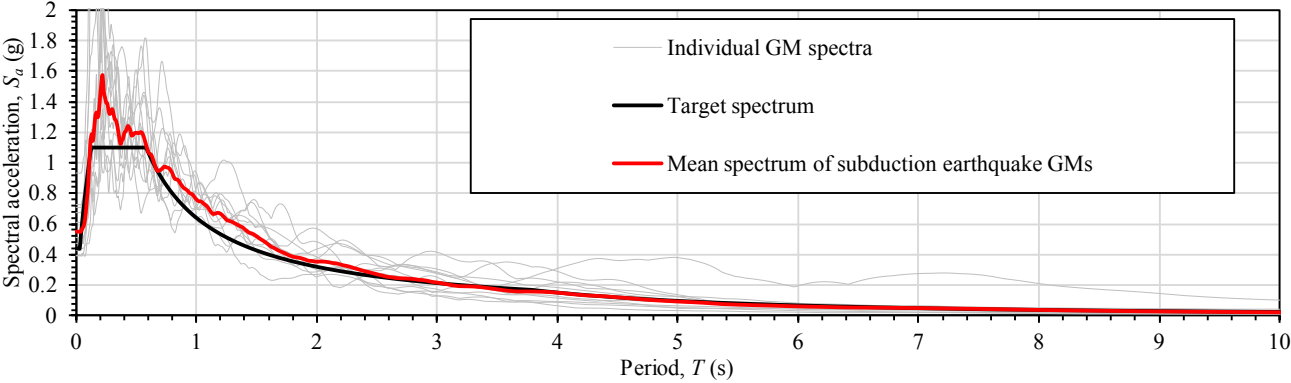


Fig. 9. Response spectra of the ground motions used in the NLRHA of the FIEBs with C-shape BIEs.

TABLE III
SELECTED GROUND MOTION RECORDS AND SCALE FACTORS FOR NLRHA

Set	GM Identification	Database	Scale factor
Crustal GMs, San José (FIEBs with W-shape and round HSS BIEs)	Northern Calif-03 (RSN-20)	[22]	2.17
	Hollister-01 (RSN-26)		5.11
	Parkfield (RSN-31)		4.8
	Managua, Nicaragua (RSN-96)		2.81
	Imperial Valley-08 (RSN-209)		5.36
	Victoria Mexico (RSN-266)		2.53
	Westmorland (RSN-317)		4.09
	Westmorland (RSN-319)		1.57
	Coalinga-01 (RSN-322)		1.88
	Coalinga-01 (RSN-342)		2.99
Subduction GMs, San José (FIEBs with W-shape and round HSS BIEs)	Coalinga-05 (RSN-412)	[23]	2.55
	HDKH070309260608		4.19
	HDKH070809110921		3.09
	IWTH151103111509		8.47
	KSRH090809110921		9.55
	TKCH080809110921		8.48
	HKD0950309260608		5.50
	HKD0950809110921		4.68
	HKD0970309260608		9.19
	HKD0970809110921		7.33
Subduction GMs, Nicoya (FIEBs with C-shape BIEs)	HKD1070309260608	[23]	9.83
	HKD1110309260608		7.69
	HKD1130309260608		14.26
	SZO0240908110507		12.63
	AOMH131103111509		4.55
	KSRH090809110921		10.84
	TKCH080809110921		10.52
	FKS0101407120422		33.99
	FKS0121407120422		24.09
	HKD0950309260608		7.93
HKD0970309260608	8.71		
HKD0970809110921	9.46		
HKD1070309260608	12.84		

B. NUMERICAL MODELLING CONSIDERATIONS

Finite element numerical models of the nine FIEBs were constructed in OpenSees [12], using force-controlled frame elements with fibre-based sections to incorporate distributed plasticity, allowing for plastic response at any point of the braces, hinging portion of the connecting knife plates, beams, and columns. The bolted knife to gusset plate connections to the beam-column joints were introduced as rigid links. The non-linear Steel02 material model, with probable yield strength, $R_y F_y$, specified for all members, was employed, and both isotropic and kinematic hardening were considered. The mass was modelled lumped at each story. A co-rotational coordinate transformation accounting for large deformations and $P-\Delta$ effects was employed to include geometric non-linearity in the analysis, and all frame members were subdivided in at least eight elements to reproduce $P-\delta$ effects with adequate accuracy. An initial out-of-straightness imperfection of one-thousandth of the member length was applied to columns, beams, and braces. In the case of the braces, this imperfection was applied such that it increased the effective eccentricity at mid-length, therefore decreasing their stiffness and strength in compression. Plane models of the SFRS alone were employed; therefore, in order to capture the destabilising $P-\Delta$ effect of the gravity loads, an auxiliary leaning column was included. This column represents the portion of the building whose mass affects the modelled FIEB and was attached with diaphragm constraints at each level. Initial Rayleigh damping of 3 % was applied to the first two modes of vibration. The acceleration histories were applied at the base of the models in the horizontal direction exclusively.

V. RESULTS AND DISCUSSION

The maximum story drift ratios recorded in the NLRHA are presented in Fig. 10. Overall, the average values of this parameter are lower than or very close to the target drift ratio of 2.0 %, which indicates that the design procedure is effective in controlling the response of the FIEBs as intended. The slight overshoot of the 4-story FIEBs with W-shape and round HSS BIEs can be attributed to the fact that most of the crustal GMs included in the analysis present spectral accelerations much larger than the design values near the fundamental period of these buildings, as can be seen in Fig. 8, which may also explain why the maximum drift ratios decrease with building height. In the case of the 4-story buildings,

the largest maximum drift ratios are observed in the first story and tend to decrease along the building height, which shows that the drift demand distribution is dominated by the fundamental mode. For the 8-story buildings, the trend is not as clear. In the case of the 12-story FIEBs, the higher mode effects result in the stories in the third quarter of the building, from bottom to top, displaying greater drift demands than the stories below for most of the GMs. As explained in [3], [4], a limitation of the design procedure employed in this study is that the displacement vector in which it relies on considers only deformation as per the fundamental mode.

In Fig. 11, the maximum story shears are presented along with the capacity-based shears for which the capacity-protected members of the FIEBs were designed. The story shears were calculated by summing the horizontal component of the internal forces in the BIEs at each story; the shear resisted by the columns is not included. Similar to what was observed for the maximum drifts, the maximum story shears are lower than or very close to the capacity-based design shears, which means that the design strength of the non-dissipating members of the SFRS is not likely to be exceeded. In the case of the three 12-story FIEBs and the 8-story FIEB with W-section BIEs, average maximum story shears slightly exceeding the design values are observed in some upper stories. This is presumably a result both of higher mode effects and of employing in the NLRHA GMs producing spectral accelerations larger than those considered in design. However, it also signals the pertinence of reviewing whether the R_y factors employed in the calculation of the probable forces developed by the BIEs could be refined, considering the differences between the response to loading of BIEs and that of the conventional members for which the R_y factors provided in ANSI/AISC 341-22 [14] were calibrated.

As an indicator of damage and potential reparability after being subject to seismic demands consistent with the design level earthquake, the residual drift ratios in the FIEBs were measured. These correspond to the state of permanent deformation present in the buildings after the end of the ground shaking. As can be observed in Fig. 12, the average residual drift ratios in all FIEBs are much smaller than the maximum drift ratios reported in Fig. 10. It showcases the partial self-centring capacity of BIEs related to their high post-elastic stiffness and to the fact that portions of the cross-section of the bracing member remain elastic even at large deformations. Moreover, the average residual drift ratios are lower than 0.5 % in all cases and indicate therefore that the damage in the buildings is likely repairable [24].

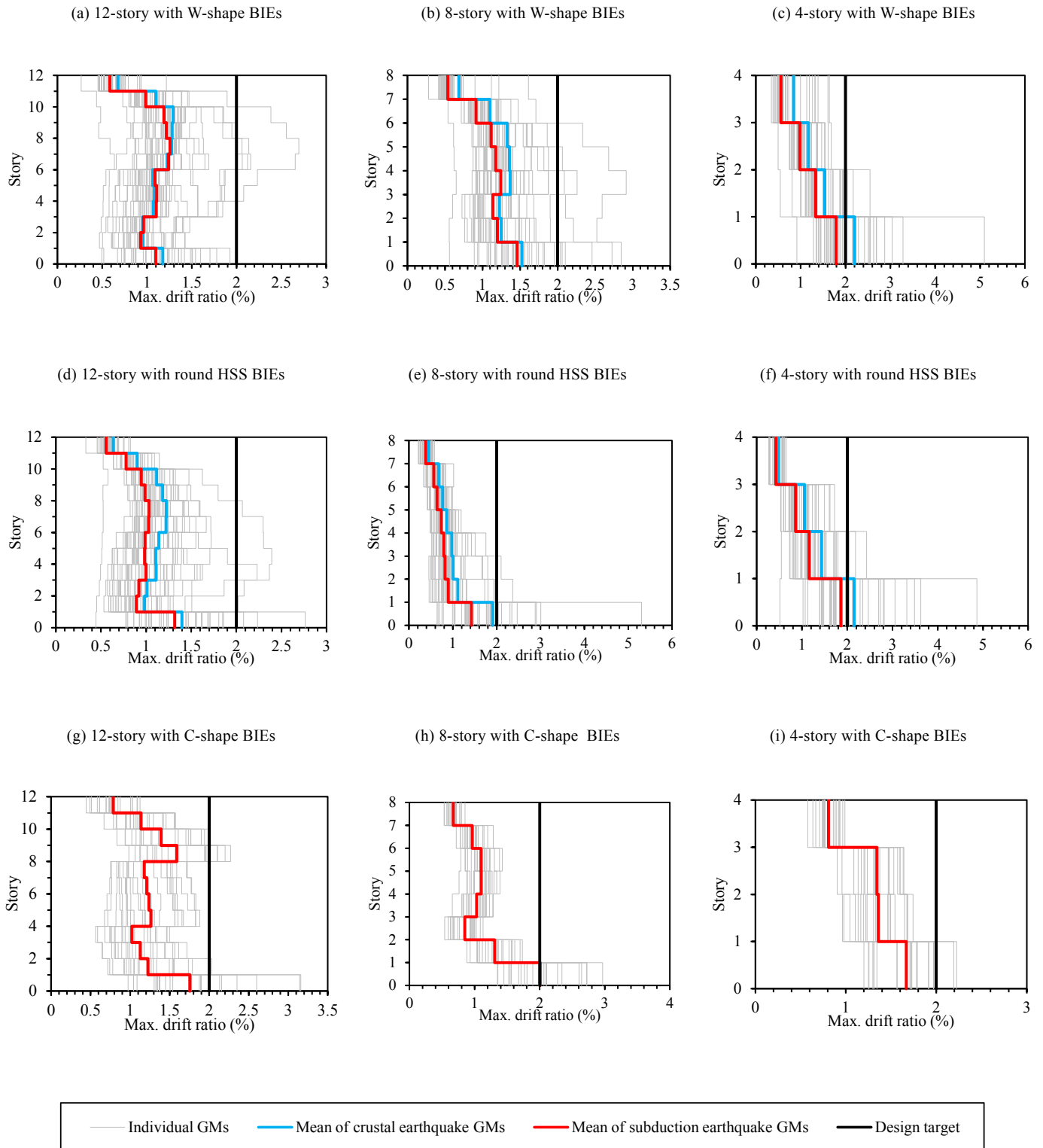


Fig. 10. Maximum story drift ratios: (a) 12-story FIEB with W-shape BIEs, (b) 8-story FIEB with W-shape BIEs, (c) 4-story FIEB with W-shape BIEs, (d) 12-story FIEB with round HSS BIEs, (e) 8-story FIEB with round HSS BIEs, (f) 4-story FIEB with round HSS BIEs, (g) 12-story FIEB with C-shape BIEs, (h) 8-story FIEB with C-shape BIEs, (i) 4-story FIEB with C-shape BIEs, and (j) legend.

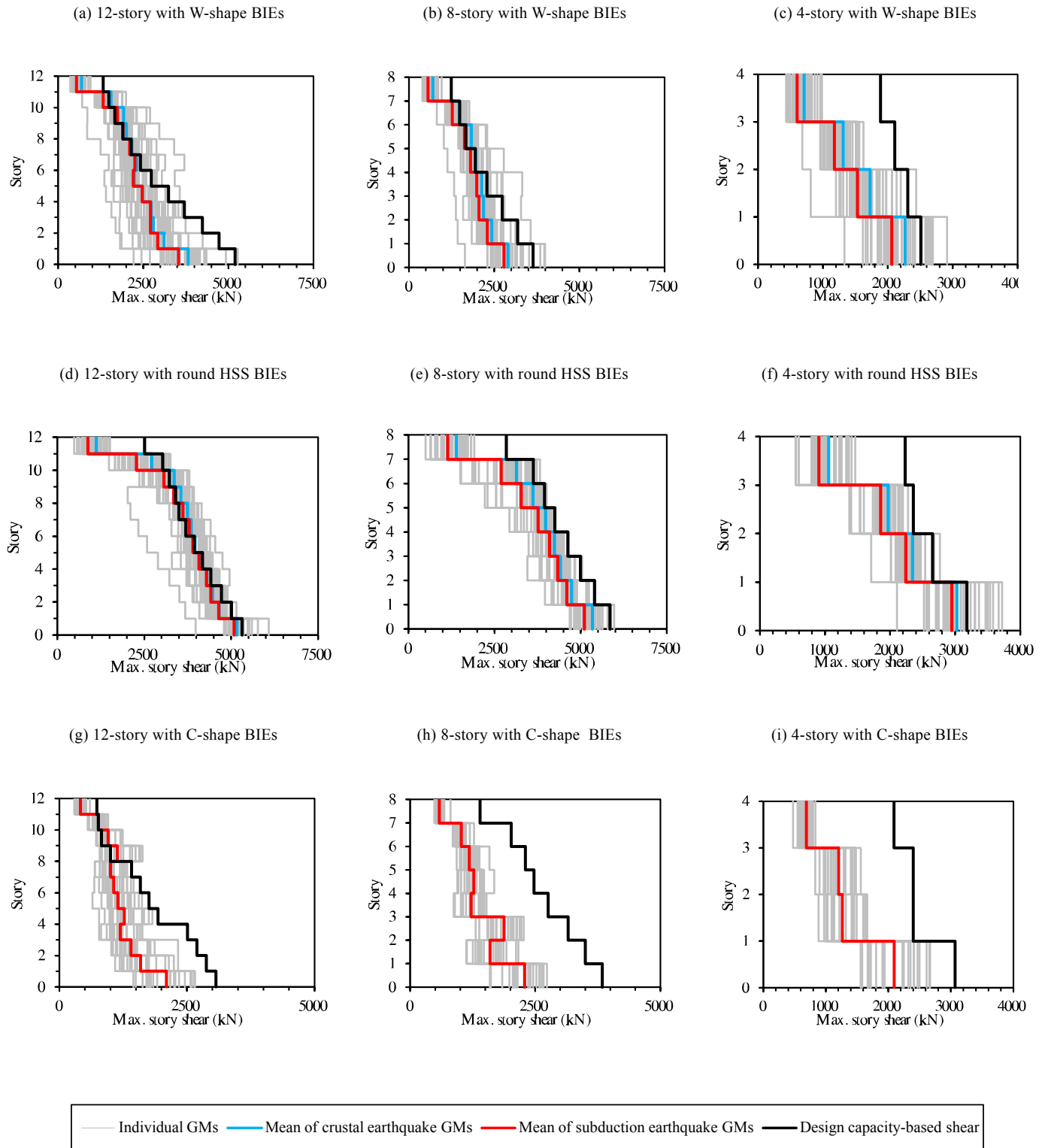


Fig. 11. Maximum story shears: (a) 12-story FIEB with W-shape BIEs, (b) 8-story FIEB with W-shape BIEs, (c) 4-story FIEB with W-shape BIEs, (d) 12-story FIEB with round HSS BIEs, (e) 8-story FIEB with round HSS BIEs, (f) 4-story FIEB with round HSS BIEs, (g) 12-story FIEB with C-shape BIEs, (h) 8-story FIEB with C-shape BIEs, (i) 4-story FIEB with C-shape BIEs, and (j) legend.

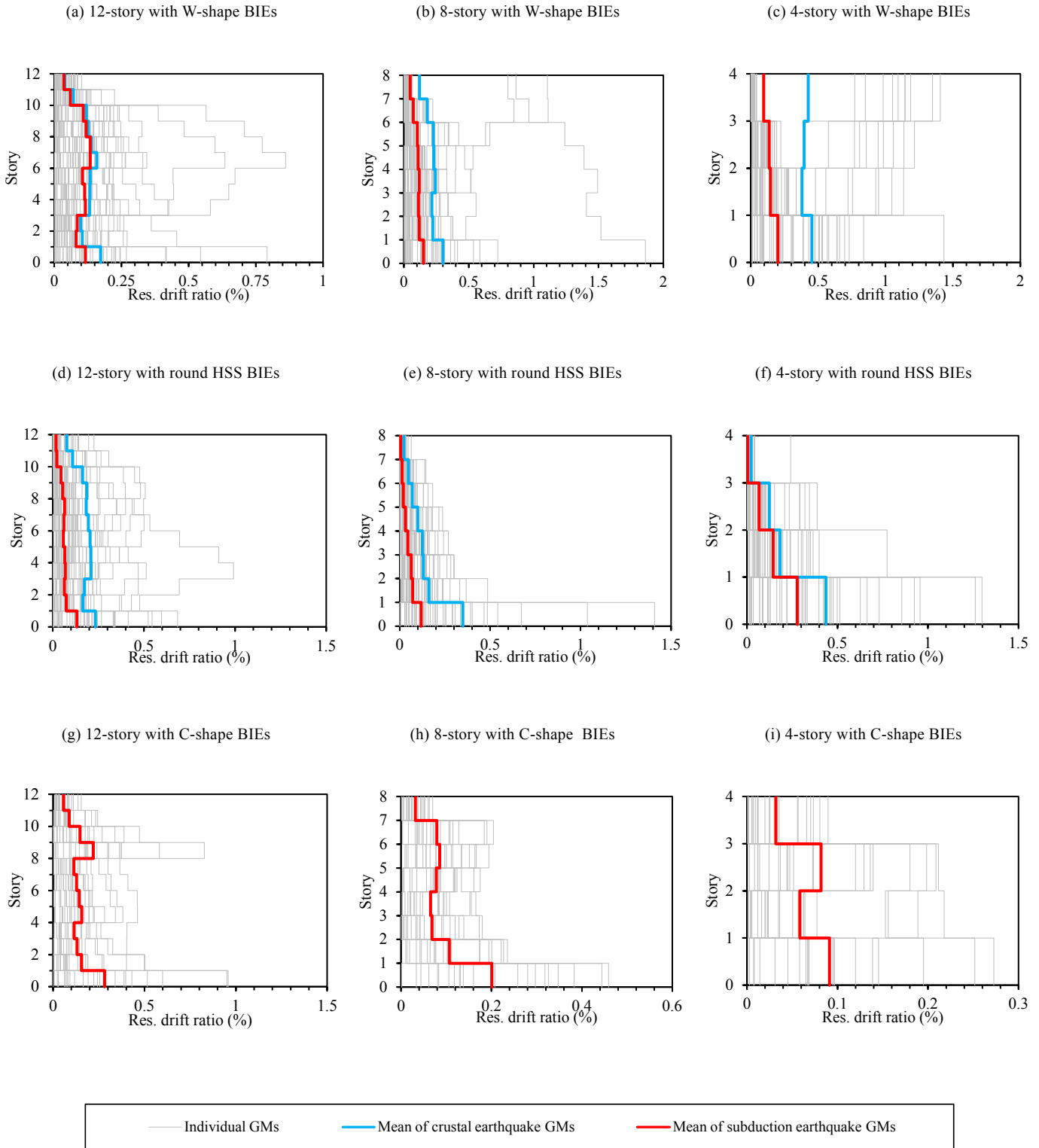


Fig. 12. Residual story drifts: (a) 12-story FIEB with W-shape BIEs, (b) 8-story FIEB with W-shape BIEs, (c) 4-story FIEB with W-shape BIEs, (d) 12-story FIEB with round HSS BIEs, (e) 8-story FIEB with round HSS BIEs, (f) 4-story FIEB with round HSS BIEs, (g) 12-story FIEB with C-shape BIEs, (h) 8-story FIEB with C-shape BIEs, (i) 4-story FIEB with C-shape BIEs, and (j) legend.

VI. CONCLUSION

The appropriateness of steel W-shapes, round HSSs, and C-shapes as bracing members in earthquake-resistant FIEBs was explored in this article. To do so, 4-, 8-, and 12-story buildings with FIEBs based on the three section types as their SFRS were first designed for the seismic hazard of Costa Rica, applying the displacement-based design procedure proposed in [3] and observing all applicable requirements from CSCR [9] and ANSI/AISC 360-22 [19]. Then, their performance under ground motions consistent with the earthquake loading considered in design was assessed through NLRHA. The main conclusions can be summarized as follows.

Firstly, all resulting buildings exhibited average maximum story drift ratios below or very close to the design target of 2.0%. This indicates that the section type employed in the BIEs does not affect the effectiveness of the displacement-based design procedure in controlling the response of FIEBs to earthquake demands consistent with the design-level seismic hazard.

Secondly, the average maximum story shears remained in most cases below the capacity-based story shears calculated as per the design procedure. Story shears exceeding by a small margin said design values were observed in the upper portion of all 12-story FIEBs and the 8-story FIEB with W-shape BIEs. These overshoots are attributed to higher mode effects, which are not explicitly regarded by the design procedure. In addition, all FIEBs displayed low residual drift ratios, with average values in all cases below 0.5%, indicating potential reparability following a severe earthquake.

Finally, among the three considered sections, the W-shapes allowed for the most cost-effective designs, owing to the low R_y factor associated with them and to the wider array of commercially available sizes. An additional advantage of employing W-shapes or C-shapes in BIEs, instead of round HSSs, is that the flat outer surface of their flanges enables the use of eccentricing assemblies simpler to fabricate.

Altogether, the results suggest that the three considered sections may be apt for use as bracing members in FIEBs. Nonetheless, these results must be complemented by further research focused on the behavior and response to loading of BIEs of the considered sections as isolated members. In particular, physical testing and high-fidelity finite element analysis of BIEs employing the sections considered in this study must be carried out to determine formally their ductility under cyclic loading and to identify all possible failure modes, in order to establish safe maximum target drift ratios for design. In addition to this, the observed overshoots in the maximum story shears signal the need of updating the design procedure to adequately incorporate the effects of higher modes of vibration.

ACKNOWLEDGMENT

This article was made possible thanks to the work of undergraduate students Daniel Martínez Vargas [5],

Willy Guerrero Angulo [6], and María José Zamora Durán [7], from the School of Civil Engineering, at Universidad de Costa Rica.

CONTRIBUTOR ROLES

Andrés González Ureña: Conceptualization, Data curation, Methodology, Project management, Resources, Software, Supervision, Validation, Visualization, Writing - of the original draft.

REFERENCES

- [1] K. A. Skalomenos, H. Inamasu, H. Shimada, and M. Nakashima, "Development of a Steel Brace with Intentional Eccentricity and Experimental Validation," *Journal of Structural Engineering*, vol. 143, no. 8, p. 04017072, Aug. 2017, doi: 10.1061/(asce)st.1943-541x.0001809.
- [2] A. González Ureña, R. Tremblay, and C. A. Rogers, "Experimental and numerical study of square HSS BIEs under cyclic loading," *Eng. Struct.*, vol. 252, p. 113669, Feb. 2022, doi: 10.1016/j.engstruct.2021.113669.
- [3] A. González Ureña, R. Tremblay, and C. A. Rogers, "Earthquake-resistant design of steel frames with intentionally eccentric braces," *J. Constr. Steel Res.*, vol. 178, p. 106483, Mar. 2021, doi: 10.1016/j.jcsr.2020.106483.
- [4] A. González Ureña, R. Tremblay, and C. A. Rogers, "Design and performance of Frames with Intentionally Eccentric Braces," in *17th World Conference on Earthquake Engineering*, Sendai, 2020.
- [5] D. Martínez Vargas, "Diseño sismorresistente de marcos de acero con riostras intencionalmente excéntricas de sección W," B.S. thesis, Escuela de Ingeniería Civil, Universidad de Costa Rica, San José, Costa Rica, 2024.
- [6] W. M. Guerrero Angulo, "Análisis numérico del comportamiento mecánico de riostras intencionalmente excéntricas con sección de acero estructural tipo C en sistemas de marcos sismorresistentes," B.S. thesis, Escuela de Ingeniería Civil, Universidad de Costa Rica, San José, Costa Rica, 2024.
- [7] M. J. Zamora Durán, "Diseño y estudio del desempeño sísmico de marcos de acero con riostras intencionalmente excéntricas con HSS circular," B.S. thesis, Escuela de Ingeniería Civil, Universidad de Costa Rica, San José, Costa Rica, 2024.
- [8] M. J. N. Priestley, G. M. Calvi, and M. J. Kowalsky, *Displacement-based seismic design of structures*. Pavia, Italy: IUSS Press, 2007.
- [9] Colegio Federado de Ingenieros y de Arquitectos de Costa Rica, *Código Sísmico de Costa Rica 2010. Revisión 2014*, Cartago, Costa Rica: Editorial Tecnológica de Costa Rica, 2014.

- [10] Standard Specification for Structural Steel Shapes, ASTM A992/A992M-22, ASTM International, Sept. 2022.
- [11] Standard Specification for High-Strength Low-Alloy Columbium-Vanadium Structural Steel, ASTM A572/A572M-21, ASTM International, Apr. 2017.
- [12] F. McKenna, M. H. Scott, and G. L. Fenves, "Nonlinear Finite-Element Analysis Software Architecture Using Object Composition," *Journal of Computing in Civil Engineering*, vol. 24, no. 1, pp. 95-107, 2010, doi: 10.1061/ASCECP.1943-5487.0000002.
- [13] *Steel Construction Manual*, 16th ed., American Institute for Steel Construction (AISC), Chicago, IL, USA, 2022.
- [14] *Seismic Provisions for Structural Steel Buildings*, ANSI/AISC 341-22, American Institute of Steel Construction (AISC), Sep. 2022.
- [15] Standard Specification for Cold-Formed Welded Carbon Steel Hollow Structural Sections (HSS), ASTM A1085/A1085M-22, ASTM International, Dec. 2022.
- [16] Standard Specification for Carbon Structural Steel, ASTM A36/A36M-19, ASTM International, Jul. 2019.
- [17] *Minimum Design Loads and Associated Criteria for Buildings and Other Structures*, ASCE/SEI 7-22, American Society of Civil Engineers (ASCE) and Structural Engineering Institute (SEI), Mar. 2022.
- [18] Canadian Commission on Building and Fire Codes, *National Building Code of Canada 2020*. Ottawa, Canada: National Research Council of Canada, 2020.
- [19] *Specification for Structural Steel Buildings*, ANSI/AISC 360-22, American Institute of Steel Construction (AISC), Aug. 2022.
- [20] D. A. Hidalgo-Leiva et al., "The 2022 Seismic Hazard Model for Costa Rica," *Bulletin of the Seismological Society of America*, vol. 113, no. 1, pp. 23-40, Dec. 2022, doi: 10.1785/0120220119.
- [21] D. Hidalgo Leiva et al., *Actualización de la Amenaza Sísmica para Costa Rica*. San José, Costa Rica: Proyecto UCREA, 2021.
- [22] T. D. Ancheta et al., "PEER NGA-West2 Database." May 2, 2013. Distributed by Pacific Earthquake Engineering Research Center. https://peer.berkeley.edu/sites/default/files/2013_03_ancheta_7.3.2020.pdf
- [23] K-NET, KiK-net, National Research Institute for Earth Science and Disaster Resilience, Nov. 2023. [Online]. Available: <https://www.kyoshin.bosai.go.jp/>
- [24] J. McCormick, H. Aburano, M. Ikenaga, and M. Nakashima, "Permissible residual deformation levels for building structures considering both safety and human elements," in *The 14th World Conference on Earthquake Engineering*, Beijing, China, 2008.